

Evidence for excimer photoexcitations in an ordered π -conjugated polymer filmK. Aryanpour,¹ C.-X. Sheng,^{2,3} E. Olejnik,² B. Pandit,² D. Psiachos,¹ S. Mazumdar,^{1,4} and Z. V. Vardeny²¹*Department of Physics, University of Arizona, Tucson, Arizona 85721, USA*²*Department of Physics, University of Utah, Salt Lake City, Utah 84112, USA*³*School of Electronic and Optical Engineering, Nanjing University of Science and Technology, Nanjing, Jiangsu 210094, China*⁴*College of Optical Sciences, University of Arizona, Tucson, Arizona 85721, USA*

(Received 28 September 2010; revised manuscript received 15 March 2011; published 28 April 2011)

We report pressure-dependent transient picosecond and continuous-wave photomodulation studies of disordered and ordered films of 2-methoxy-5-(2-ethylhexyloxy) poly(para-phenylenevinylene). Photoinduced absorption (PA) bands in the disordered film exhibit very weak pressure dependence and are assigned to intrachain excitons and polarons. In contrast, the ordered film exhibits two additional transient PA bands in the midinfrared that blueshift dramatically with pressure. Based on high-order configuration interaction calculations, we ascribe the PA bands in the ordered film to excimers. Our work brings insight to the exciton binding energy in ordered films versus disordered films and solutions. The reduced exciton binding energy in ordered films is due to energy states appearing below the continuum band threshold of the single strand.

DOI: [10.1103/PhysRevB.83.155124](https://doi.org/10.1103/PhysRevB.83.155124)

PACS number(s): 78.47.-p, 71.35.Cc, 78.30.Jw, 78.55.Kz

I. INTRODUCTION

Ordered π -conjugated polymer (PCP) films exhibit photophysics remarkably different from dilute solutions or disordered films.¹⁻⁴ Explanations given for these differences include photoexcitation branching into intrachain excitons and polarons in the ordered films,⁵ as well as the formation of a variety of intermolecular species such as polaron pairs,¹⁻³ aggregates,^{1,4,6} and excimers.⁷⁻¹⁰ Although our understanding of the photophysics due to these interchain species is incomplete, it is generally agreed that the distinctive behavior of the ordered films are due to strong interchain interactions absent in dilute solutions or disordered films. It follows therefore that the ability to vary interchain interactions in a controlled manner should provide an ideal tool for understanding the role of morphology in the photophysics of these materials.

In the present paper we report such a study: we probe pressure effects on the transient picosecond and continuous wave (cw) photomodulation (PM) spectra of disordered and ordered 2-methoxy-5-(2-ethylhexyloxy) poly(para-phenylenevinylene) (MEH-PPV) films up to 119 kbar. The ordered film exhibits two correlated photoinduced absorption (PA) bands absent in the disordered films, which dramatically blue-shift with pressure. We present correlated-electron calculations of excited-state absorptions from interacting chains that establish that such blueshift of PA bands is not expected from aggregates or polaron pairs. Our calculations establish unambiguously that the primary photoexcited species in ordered MEH-PPV films are excimers, whose PA bands are expected to show pressure-induced blueshift. Specifically, the blueshift indicates pressure-induced changes in the wave functions of the initial and final states of these PA bands. We show that such changes in turn indicate nonzero but incomplete intermolecular charge transfer in the initial state of the excited-state absorption, as occurs only in the excimer.

In Sec. II we describe our experimental details and results. Following this, in Secs. III and IV we discuss our theoretical approach and computational results. Finally in Sec. V we present our conclusions. Although we are primarily interested

in determining the nature of the interchain species in ordered MEH-PPV films, our work also has implications for the exciton binding energy in PCP films. The magnitude of the exciton binding energy in PCPs is a controversial quantity. Our work brings new insight to this subject.

II. EXPERIMENT

We used thin films of polymer samples drop-cast from powder as received from American Dye Service (ADS). Transient PM spectroscopy was utilized to resolve the primary photoexcitations. Specifically, we used a femtosecond two-color pump-probe correlation technique with a low-power (energy per pulse ~ 0.1 nJ), high-repetition-rate (~ 80 MHz) laser system based on a Ti:sapphire (Tsunami, Spectra-Physics) laser having a temporal pulse resolution of 150 fs.¹¹ The pump $\hbar\omega$ was frequency doubled to $\hbar\omega = 3.1$ eV and we used the output beam of an optical parametric oscillator as the probe $\hbar\omega$ from 0.24 to 1.1 eV.¹¹ The pump and probe beams were focused on the film surface inside the pressure cell to a spot ~ 100 μm in diameter. The transient PM signal was measured using a phase-sensitive lock-in technique at modulation frequency of 30 kHz provided by an acousto-optic modulator. In the mid-IR spectral range we only obtained PA, which is given as the fractional change in transmission, $\Delta T/T(t)$. Both T and ΔT were measured using solid-state photodetectors, namely Ge, InSb, and MCT depending on the spectral range of interest. We carefully aligned the pump and probe beams to reduce the *beam walk* in the experiment. For the steady-state PM spectra, we employed a cw laser for pump excitation (Ar⁺ laser) and an incandescent light (Tungsten Halogen lamp) as a probe,¹² using a standard PM setup based on a $\frac{1}{4}$ -m monochromator or Fourier transform infrared (FTIR) spectrometer. The pump beam intensity was 100 mW/cm² and the probe beam was prefiltered to eliminate excitation above the film's optical gap. We used a modulation frequency of 350 Hz having a peak sensitivity for photoexcitations with about 1 ms lifetime. Solid-state detectors such as Si, Ge, and InSb spanned the probe photon energy from 0.25 to 2.2 eV.

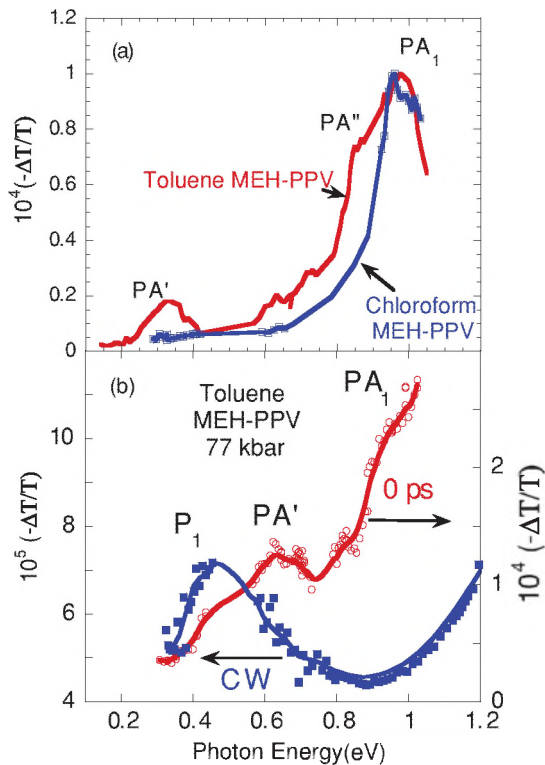


FIG. 1. (Color online) (a) Transient picosecond PM spectra at $t = 0$ of MEH-PPV(T) (red) and MEH-PPV(C) (blue) films. The exciton PA_1 band and excimer PA' and PA'' bands are assigned. (b) Transient (red) and cw (blue) PM spectra of MEH-PPV(T) at hydrostatic pressure of 77 kbar. PA_1 and PA' are as in (a); P_1 is a polaron band.

Figure 1(a) shows the transient PM spectra at time $t = 0$ of two MEH-PPV(T) and MEH-PPV(C) films cast from toluene and chloroform solutions, respectively. Since toluene is a poor solvent for MEH-PPV,^{1,4} MEH-PPV(T) films contain coexisting ordered and disordered phases.¹ MEH-PPV(C) contains predominantly the disordered phase.^{1,4} The transient PM of the MEH-PPV(C) contains a single PA band, PA_1 , which peaks at ~ 0.95 eV, very similar to PA_1 of MEH-PPV in solution, and is correlated to the stimulated emission band

in the visible spectral range.¹¹ We therefore identify it as being due to intrachain excitons. The MEH-PPV(T) shows two *additional* PA bands, PA' at ~ 0.35 eV and a shoulder PA'' at ~ 0.85 eV. We assign these bands to interchain species.

The band PA' in MEH-PPV was identified previously as being due to polarons,¹¹ since the cw polaron band P_1 also peaks at about the same value, $\hbar\omega(\text{probe}) = 0.4$ eV.¹³ To confirm the assignment of PA' to interchain species, we applied high hydrostatic pressure P to the MEH-PPV(T) film in a pressure cell. The MEH-PPV film was peeled off the substrate under a microscope and placed in a diamond-anvil cell equipped with IR-transmitting windows that was filled with a pressure-transmitting liquid, perfluorotributylamine, to ensure hydrostatic pressure. The pressure inside the cell was measured via the pressure-induced blueshift in the polymer IR-active C-H frequency at ~ 3000 cm^{-1} , which was precalibrated against the pressure-induced change of the well-known photoluminescence (PL) lines of a ruby chip. Figure 1(b) shows the transient and cw PM spectra under pressure $P = 77$ kbar. PA' blueshifts substantially to ~ 0.65 eV, in contrast to the polaron P_1 band in the cw PM spectrum, which does not shift with pressure [Fig. 2(b)]. PA' is therefore not due to polarons.

Figure 2(a) shows the MEH-PPV transient PM spectrum for various increasing P values. PA' and PA'' both grow in intensity relative to PA_1 , and also blueshift together, whereas PA_1 remains at ~ 0.95 eV. The energy shifts of PA_1 , PA' , and cw P_1 due to polarons are plotted versus P up to 120 kbar in Fig. 2(b). PA' shifts by about 0.35 eV up to $P = 77$ kbar, and it peaks at the same $\hbar\omega(\text{probe})$ at still higher P ; in contrast, P_1 and PA_1 do not shift much with pressure. Figure 2(c) shows the decay dynamics of PA' and PA'' at $P = 119$ kbar. The dynamics are clearly identical, coming from the same photoexcitation species.

III. THEORETICAL MODEL AND PARAMETRIZATION

We model the ordered phase as two interacting, cofacially stacked, planar PPV oligomers of equal length.^{14,15} Previously we have shown that high-order configuration interaction (CI) calculations inclusive of all quadruple excitations are essential for finding the PA' band.¹⁴ This necessitates the

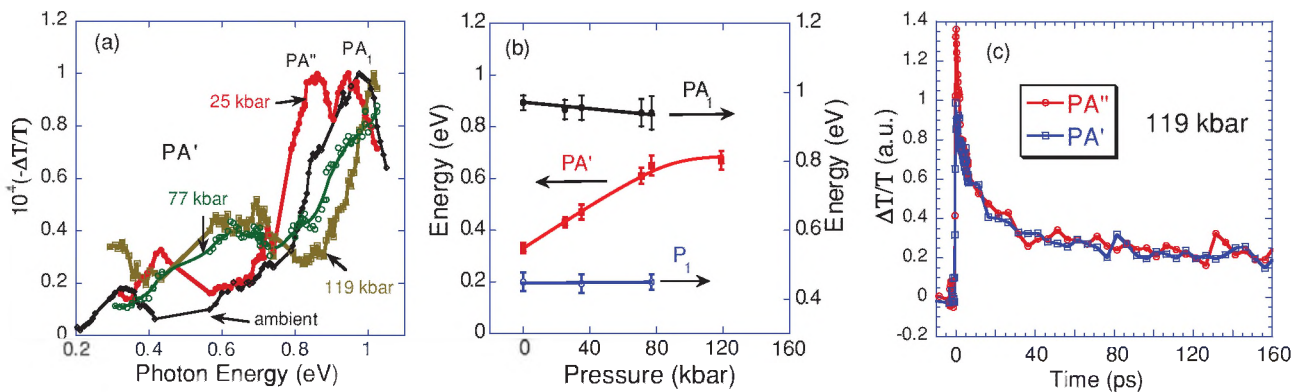


FIG. 2. (Color online) (a) Picosecond transient ($t = 0$) PM spectra of MEH-PPV(T) at ambient pressure, and $P = 25$, 77, and 119 kbar; the PA bands are assigned as in Fig. 1. (b) Summary of the peak positions for the transient PA' (red) and PA_1 (black) at $t = 0$; and cw P_1 (blue) vs P . (c) The decay dynamics of the transient PA' and PA'' bands at $P = 119$ kbar.

use of the semiempirical π -electron Hamiltonian and also limits the lengths of our oligomers to three units. Even with such a small system size for the two-chain system, our basis size is 1.8 million. For computational simplicity we chose a symmetric arrangement, where each carbon atom of one oligomer lies directly on top of the equivalent carbon atom of the second oligomer. Our calculations are based on the Hamiltonian $H = \sum_{\mu=1,2} H_{\mu} + H_{\mu,\mu'}$, where H_{μ} is the single-chain Pariser-Parr-Pople Hamiltonian,¹⁶

$$H_{\mu} = - \sum_{\langle ij \rangle, \sigma} t_{ij} (c_{\mu,i,\sigma}^{\dagger} c_{\mu,j,\sigma} + \text{H.c.}) + \sum_i U n_{\mu,i,\uparrow} n_{\mu,i,\downarrow} + \sum_{i < j} V_{ij} (n_{\mu,i} - 1) (n_{\mu,j} - 1). \quad (1)$$

Here $c_{\mu,i,\sigma}^{\dagger}$ creates a π electron of spin σ on carbon atom i of the μ th molecule, $n_{i,\mu,\sigma} = c_{\mu,i,\sigma}^{\dagger} c_{\mu,i,\sigma}$ and $n_{\mu,i} = \sum_{\sigma} n_{i,\mu,\sigma}$. We chose the nearest-neighbor hopping matrix element $t_{ij} = t = 2.4$ eV for phenyl C–C bonds, and 2.2 (2.6) eV for the intrachain single (double) C–C bonds.¹⁷ The variable U is the repulsion between two electrons occupying the same p_z orbital of a C atom, and V_{ij} are intrachain intersite Coulomb interactions parametrized as $V_{i,j} = U / (\kappa \sqrt{1 + 0.6117 R_{ij}^2})$, where R_{ij} is the distance between C atoms i and j in angstroms. We chose $U = 8.0$ eV and $\kappa = 2$.¹⁷

The intermolecular Hamiltonian is written as¹⁴

$$H_{\mu,\mu'} = - \sum_{\langle ij \rangle, \sigma} t_{ij}^{\perp} (c_{\mu,i,\sigma}^{\dagger} c_{\mu',j,\sigma} + \text{H.c.}) + \sum_{i < j} V_{ij}^{\perp} (n_{\mu,i} - 1) (n_{\mu',j} - 1), \quad (2)$$

where $t_{ij}^{\perp} = t^{\perp}$ is restricted to nearest neighbors. For V_{ij}^{\perp} we chose the same functional form as V_{ij} , with a screening parameter $\kappa^{\perp} \leq \kappa$.¹⁸ We report calculations for $\kappa^{\perp} = \kappa = 2$. Our basis set consists of Hartree-Fock (HF) orbitals localized on individual molecules, allowing calculation of the total charge on the individual oligomers (hereafter ionicity ρ) for each eigenstate.

Both the interaction and the hopping terms in $H_{\mu,\mu'}$ change with pressure. There is no *ab initio* approach to determine these changes. On the other hand, our goal is to understand the effects of enhanced pressure, at a qualitative level only, that would allow comparisons between the PA bands expected from the different kinds of intermolecular species. We modeled the effects of increasing pressure by decreasing the intermolecular distance from 0.41 nm at ambient pressure to 0.37 nm at the highest pressures, while increasing t^{\perp} from 0.07 to 0.15 eV. In addition to reducing intermolecular distances, pressure also causes planarization of individual chains,¹⁹ which can have two different consequences. First, planarization can increase the effective conjugation length, which in turn primarily decreases intramolecular transition energies. This is not of interest here, because our focus is on intermolecular interactions. A second consequence of increased planarization is enhanced t^{\perp} , an effect that we have included.

IV. COMPUTATIONAL RESULTS

The intermolecular species we investigated are (i) the delocalized covalent ($\rho = 0$) optical exciton $|\text{exc}_1\rangle + |\text{exc}_2\rangle$, where $|\text{exc}_j\rangle$ implies excitation on the j th molecule; (ii) the completely ionic ($\rho = 1$) Coulombically bound polaron pair $|P_{\mu}^{+} P_{\mu'}^{-}\rangle$, where $P_{\mu}^{+} (P_{\mu'}^{-})$ is a positively (negatively) charged oligomer¹⁻³; and (iii) the excimer or charge-transfer exciton,^{7,8,10,14,20} $|\text{CTX}\rangle$,

$$|\text{CTX}\rangle = c_c (|\text{exc}_1\rangle - |\text{exc}_2\rangle) + c_i (|P_1^{+} P_2^{-}\rangle - |P_2^{+} P_1^{-}\rangle) + \dots, \quad (3)$$

where the centered ellipsis denotes higher-order terms; for $|\text{CTX}\rangle$, $0 < \rho < 1$. In all our calculations with the parameters as stated above we have found $|\text{CTX}\rangle$ to be the lowest excited state, with the polaron pair $|P_{\mu}^{+} P_{\mu'}^{-}\rangle$ occurring above the optical exciton.

With completely equivalent PPV oligomers, the polaron pair is thus never the lowest state at the optical edge and occurs above the optical exciton.¹⁴ Since we are interested only in PA from the polaron pair, which in turn depends only on its wave function and not how it is created, we create the polaron pair by making the PPV oligomers inequivalent. This is done by lowering all HF molecular orbital energies of one oligomer with respect to the other by a fixed energy 2ϵ (in effect creating a heterostructure). For $\epsilon = 0.185$ eV and $\kappa^{\perp} = 1.3$, the lowest excited state of the two-chain system is the polaron pair with $\rho = 0.9$.¹⁸

Figure 3(a) shows our calculated PA₁ band of the optical exciton for the two-chain system as a function of decreasing interchain distance and increasing interactions. Here and in Figs. 3(b) and 3(c) we scaled all excitation energies by the energy E_{1B_n} of the single-chain exciton for comparison to experiments. PA₁ exhibits a weak redshift at the highest t^{\perp} , in contrast to the blueshift of the PA'' band. Our calculated PA bands from the polaron-pair state [see Fig. 3(b)] are not affected at all by the increased intermolecular interaction. Thus, the PA' and PA'' bands in the picosecond transient PM spectra of the ordered films cannot be ascribed to excitons or polaron pairs.

In Fig. 3(c) we show the calculated PA bands from $|\text{CTX}\rangle$, which is the lowest excited state of our Hamiltonian, for several different $H_{\mu,\mu'}$. The lowest-energy PA₀ lies outside our experimental spectral range,¹⁴ whereas PA' and PA'' are both seen in the experiment. PA' (PA'') originates predominantly from the polaron-pair (exciton) component of $|\text{CTX}\rangle$. The pressure-induced blueshifts of the experimental PA' and PA'' energies shown in Fig. 2(a) are replicated in Fig. 3(c). Although quantitative comparisons are difficult, with $E_{1B_n} \sim 2.2$ eV for MEH-PPV the scaled energy shift of the PA' band at the largest $H_{\mu,\mu'}$ is about 0.25 eV, which is close to the maximum measured blueshift of this band shown in Fig. 2(a) (~ 0.3 eV).

The weak pressure effect on the optical exciton and polaron-pair PA is due to their extreme ionicities, $\rho = 0$ and 1, respectively, that do not change with pressure. In Figs. 4(a) and 4(b) we give a mechanistic explanation for the observed blueshifts of the excimer PA bands under pressure. Increased $H_{\mu,\mu'}$ leads to a significant decrease in the energy of $|\text{CTX}\rangle$ [see Fig. 4(a)] as a consequence of its

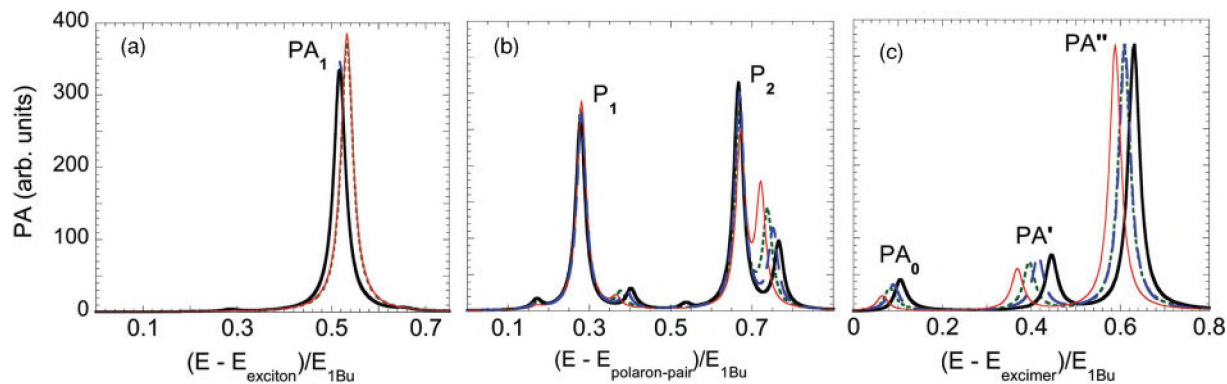


FIG. 3. (Color online) (a) Calculated dependence of PA bands from (a) the two-chain exciton, (b) the polaron pair, and (c) the excimer, on intermolecular interactions. Thin (red) curves represent $t^\perp = 0.07$ eV, intermolecular separation $d = 0.41$ nm; dotted (green) curves represent $t^\perp = 0.1$ eV, $d = 0.4$ nm; dashed (blue) curves represent $t^\perp = 0.12$ eV, $d = 0.38$ nm; and thick (black) curves represent $t^\perp = 0.15$ eV, $d = 0.37$ nm.

increased ionicity [see Fig. 4(b)]. Our calculated ρ for the final state of PA' is considerably larger than ρ for [CTX] [see Fig. 4(b)], indicating that the PA' absorption, over and above intramolecular polaronlike excitations, also receives a strong contribution from intermolecular charge-transfer excitation. Furthermore, even as the energy of the excimer decreases and its ionicity increases, the energy of the final state of PA' increases [see Fig. 4(a)] while its ionicity decreases [see Fig. 4(b)]. This indicates that the charge-transfer component of PA' increases with increasing $H_{\mu,\mu'}$ (and hence with increasing pressure). In contrast to the final state of PA', the final state of PA'' has a very small ionicity [see Fig. 4(b)], indicating that PA'' excitation is from the neutral exciton component of [CTX]. Hence, the increase in PA'' peak energy comes mostly from the decrease in [CTX] energy with P . As seen in Fig. 4(a), the energy of the final state of PA'' is nearly independent of t^\perp and actually decreases weakly with increasing t^\perp .

Our analyses in Fig. 3(c) give insight into the smaller exciton binding energies in ordered films than in solutions of PCPs.²¹ The experimentally measured exciton binding energy is the energy difference between the lowest state with a free electron and hole and the bound optical exciton. In solutions and disordered films, these states are eigenstates of H_μ alone.

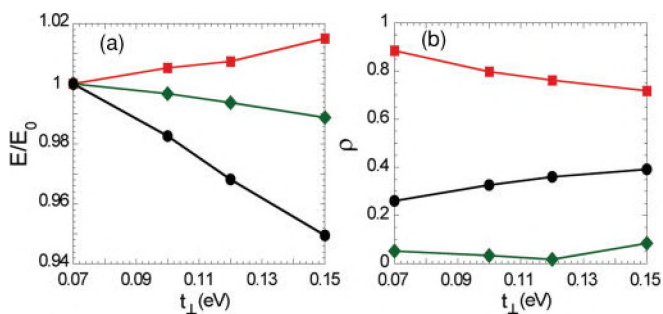


FIG. 4. (Color online) (a) Energies (E) of the excimer [(black) circles], the final state of PA' [(red) squares], and the final state of PA'' [(green) diamonds] as a function of t^\perp , normalized by the energies E_0 of the same states at $t^\perp = 0.07$ eV (ambient pressure). The interchain distances d corresponding to each t^\perp are the same as in Fig. 3. (b) Ionicities of the states in (a).

The threshold of the continuum band in the single chain, referred to as nB_u , occurs slightly above a two-photon mA_g exciton in which intrachain charge separation is much larger than in the optical $1B_u$ exciton (see Fig. 12 in Ref. 22). The PA band PA₁ corresponds to the excited-state absorption from the $1B_u$ to the mA_g , while the nB_u is reached upon further intrachain charge separation.²² In contrast, excited states in ordered films are eigenstates of the *complete* Hamiltonian $H_\mu + H_{\mu,\mu'}$. Our wave-function analysis shows that PA' from the excimer is to a two-photon exciton state with much larger *interchain* charge transfer than the excimer. The final state of PA' is thus the exact many-chain equivalent of the mA_g in single chains. For interacting chains, therefore, *interchain charge separation is energetically less costly*, and it is very likely that further charge separation is also interchain; hence the observed smaller exciton binding energy in ordered films²¹ is most probably due to the appearance of new low-lying states with greater charge separation below the single-chain continuum and not because the mA_g or the nB_u comes down in energy due to screening in interacting chains. A complete proof requires quadruple CI calculations of very high energy excited states for multiple (greater than two) chains, which is beyond

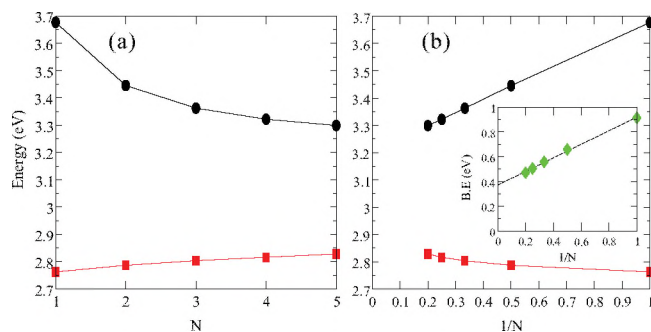


FIG. 5. (Color online) SCI continuum band threshold energy [(black) circles] and the exciton energy [(red) squares] vs (a) N and (b) $1/N$, where N is the number of interacting eight-unit PPV oligomers. The distance between the chains is 0.4 nm and the interchain hopping is $t^\perp = 0.1$ eV. The inset [(green) diamonds] in (b) shows the exciton binding energy as a function of $1/N$, with 0.4 eV as the $N \rightarrow \infty$ extrapolated value.

current computational capability. We present below the results of approximate calculations that support this conjecture.

Unlike the even-parity two-photon state that is the final state of PA', the optical exciton as well as the continuum band threshold state are odd-parity one-photon states. It is known that they can therefore be determined semiquantitatively from approximate single CI (SCI) calculations.¹⁷ This remains true independent of the number of chains. The threshold of the continuum band within the SCI is the HF gap.¹⁷ We have calculated the HF gap and the SCI optical exciton energy within our Hamiltonian for eight-unit PPV oligomers, for up to five chains. We show these quantities plotted against N in Fig. 5(a) and against $1/N$ in Fig. 5(b), where N is the number of oligomers. The convergence with increasing number of oligomers is obvious from Fig. 5(a). (The small increase in the energy of the optical exciton is expected and is due to nonzero exciton bandwidth, with the optical exciton occurring at the top of the band, as in a H aggregate.¹⁴) The inset of Fig. 5(b) shows the exciton binding energy versus $1/N$. The $N \rightarrow \infty$ extrapolated exciton binding energy is nearly half of that in the single-chain limit. Importantly, this decrease in exciton binding energy of the many-chain system occurs in spite of PA₁, which gives the lower limit of the exciton binding energy in the single-chain limit,¹⁷ continuing to occur at much higher energy [see Figs. 2(a) and 3(a)]. Thus, the reduction in the exciton binding energy is due to the appearance of new states that are absent in the single-chain limit. Excitonic states derived from the single chain continue to occur above the many-chain continuum band threshold. We previously reproduced the observed absorption spectrum of PPV¹⁷ and the energies of the mA_g and the lowest spin triplet nearly

quantitatively with our Coulomb parameters.²³ It is interesting that our extrapolated many-chain exciton binding energy in Fig. 5(b) is very close to the experimental value for PPV films.²¹

V. CONCLUSIONS

In summary, the significant pressure-induced blueshifts exhibited by the transient PA bands in ordered MEH-PPV films indicate *intermediate ionicity for the primary photoexcitation*, i.e., an excimer. PA bands of the optical exciton with ionicity 0, and of the polaron pair with ionicity nearly 1, are unaffected by pressure. Understanding the role of morphology in the photophysical behavior of PCP films is crucial for their applications in next-generation optoelectronic devices. Our joint theory-experiment work provides a diagnostic tool for the investigation of the nature of the primary photoexcitations in polymer films, with potentially wide applications in other polymer physics areas.

ACKNOWLEDGMENTS

The Utah group thanks Valentina Morandi and Josh Holt for help with the high-pressure and picosecond measurements. The work at Utah was supported in part by NSF Grant No. DMR-0803325. The Arizona group thanks Alok Shukla and Zhendong Wang for computational help. The work at Arizona was partially supported by NSF Grant No. DMR-0705163. C.-X.S. thanks the support of National Natural Science Foundation of China Grant No. 61006014, NUST research funding 2010ZDJH03 and the "Zijin star" project.

¹L. Rothberg, in *Photophysics of Conjugated Polymers, Semiconducting Polymers: Chemistry, Physics and Engineering*, edited by G. Hadziioannou and G. G. Malliaras (Wiley, New York, 2006), Vol. I, pp. 179–204.

²V. I. Arkhipov and H. Bassler, *Phys. Status Solidi A* **201**, 1152 (2004).

³E. M. Conwell, in *Organic Electronic Materials: Conjugated Polymers and Low Molecular Weight Solids*, edited by R. Farchioni and G. Grosso (Springer, New York, 2001), pp. 127–180.

⁴B. J. Schwartz, *Annu. Rev. Phys. Chem.* **54**, 141 (2003).

⁵P. B. Miranda, D. Moses, and A. J. Heeger, *Phys. Rev. B* **64**, 081201 (2001).

⁶J. Clark, C. Silva, R. H. Friend, and F. C. Spano, *Phys. Rev. Lett.* **98**, 206406 (2007).

⁷S. A. Jenekhe and J. A. Osaheni, *Science* **265**, 765 (1994).

⁸S. Webster and D. N. Batchelder, *Polymer* **37**, 4961 (1996).

⁹R. Jakubiak, C. J. Collison, W. C. Wan, and L. J. Rothberg, *J. Phys. Chem. A* **103**, 2394 (1999).

¹⁰S. Singh, T. Drori, and Z. V. Vardeny, *Phys. Rev. B* **77**, 195304 (2008).

¹¹C.-X. Sheng, M. Tong, S. Singh, and Z. V. Vardeny, *Phys. Rev. B* **75**, 085206 (2007).

¹²X. M. Jiang, R. Osterbacka, O. Korovyanko, C. P. An, B. Horovitz, R. A. J. Janssen, and Z. V. Vardeny, *Adv. Funct. Mater.* **12**, 587 (2002).

¹³T. Drori, E. Gershman, C. X. Sheng, Y. Eichen, Z. V. Vardeny, and E. Ehrenfreund, *Phys. Rev. B* **76**, 033203 (2007).

¹⁴Z. Wang, S. Mazumdar, and A. Shukla, *Phys. Rev. B* **78**, 235109 (2008); D. Psiachos and S. Mazumdar, *ibid.* **79**, 155106 (2009).

¹⁵Y.-S. Huang, S. Westenhoff, I. Avilov, P. Sreearunothai, J. M. Hodgkiss, C. Deleener, R. H. Friend, and D. Beljonne, *Nat. Mater.* **7**, 483 (2008).

¹⁶R. Pariser and R. G. Parr, *J. Chem. Phys.* **21**, 9865 (1953); J. A. Pople, *Trans. Faraday Soc.* **49**, 767 (1953).

¹⁷M. Chandross, S. Mazumdar, M. Liess, P. A. Lane, Z. V. Vardeny, M. Hamaguchi, and K. Yoshino, *Phys. Rev. B* **55**, 1486 (1997).

¹⁸K. Aryanpour, D. Psiachos, and S. Mazumdar, *Phys. Rev. B* **81**, 085407 (2010).

¹⁹J. P. Schmidtke, J. S. Kim, J. Gierschner, C. Silva, and R. H. Friend, *Phys. Rev. Lett.* **99**, 167401 (2007).

²⁰H. Marciniak, M. Fiebig, M. Huth, S. Schiefer, B. Nickel, F. Selmaier, and S. Lochbrunner, *Phys. Rev. Lett.* **99**, 176402 (2007).

²¹R. N. Marks, J. J. M. Halls, D. D. C. Bradley, R. H. Friend, and A. B. Holmes, *J. Phys. Condens. Matter* **6**, 1379 (1994); S. Barth and H. Bässler, *Phys. Rev. Lett.* **79**, 4445 (1997).

²²M. Chandross, Y. Shimoi, and S. Mazumdar, *Phys. Rev. B* **59**, 4822 (1999).

²³M. Chandross and S. Mazumdar, *Phys. Rev. B* **55**, 1497 (1997).